EUROPEAN ORGANIZATION FOR NUCLEAR RESEARCH

Proposal to the ISOLDE and Neutron Time-of-Flight Committee

Investigating the origins of the kink in charge radii at N=28

01.10.2024

A. Antušek[1], N. Azaryan[2], M. Baranowski[3], M. Bissell[2], M. Chojnacki[2], J. Dobaczewski[4], J. Ginges[6], R. de Groote[7], R. Han[8], A. Hurajt[9], M. Kortelainen[8], A. Koszorous[7], M. Kowalska[2], I. Michelon[2], A. Nagpal[2], D. Paulitsch[2], M. Pešek[2], M. Piersa-Siłkowska[2], B. Roberts[6], A. Sparks[2], H. Wibowo[4] and D. Zakoucky[10].

[1]*Faculty of Materials Science and Technology, Slovak University of Technology, 917 24 Trnava, Slovak Republic*

[2]*Experimental Physics Department, CERN, 1211 Geneva, Switzerland*

[3]*Faculty of Physics, Adam Mickiewicz University, 61-614 Poznań, Poland*

[4]*Department of Physics, University of York, Heslington, York YO10 5DD, United Kingdom*

[5]*Institute of Theoretical Physics, Faculty of Physics, University of Warsaw, ul. Pasteura 5, PL-02-093 Warsaw, Poland*

[6]*School of Mathematics and Physics, The University of Queensland, Brisbane QLD 4072, Australia*

[7]*KU Leuven, Instituut voor Kern- en Stralingsfysica, Leuven, Belgium*

[8]*Department of Physics, University of Jyväskylä, Accelerator Laboratory, P.O. Box 35, FI-40014, Jyväskylä, Finland*

[9]*Department of Physical and Theoretical Chemistry, Faculty of Natural Sciences, Comenius University in Bratislava, Mlynskádolina, Ilkovičova 6, 842 15 Bratislava, Slovak Republic*

[10]*Nuclear Physics Institute, Acad. Sci. Czech Rep., CZ-25068, Rez, Czech Republic*

Spokespersons: M. L. Bissell, M. Kowalska
Contact person: M. L. Bissell

CERN-INTC-2024-058 / INTC-P-714
02/10/2024

Abstract:

Charge radii of neutron-rich isotopes in the calcium region show a distinctive increase in slope or "kink" at *N*=28. Although expected when crossing a shell closure, the size of the kink cannot be explained by most nuclear structure calculations. What is thus the source of this enhanced kink? Is it increased deformation or maybe a significantly larger radial extent of neutron orbits, as suggested by some theoretical studies?

To address these questions, we propose to measure the quadrupole moment of ^{48}K (*N*=29) and its differential 'hyperfine anomaly' compared to odd-even neighbours ^{47}K and ^{49}K. The hyperfine anomaly will be determined based on the precise measurements of $^{47\text{-}49}$K magnetic moments (using β-NMR) and their hyperfine structure constants (using laser-rf double resonance spectroscopy). The results will be interpreted using state of the art nuclear-structure and atomic-wavefunction calculations.

Summary of requested shifts: 21 shifts + 9 offline shifts, (split into 3 runs over 1 year)

Motivation

Laser spectroscopy experiments in the Calcium region [1,2] discovered a dramatic increase in rms nuclear charge radii after neutron number 28. This behaviour is particularly surprising given the evidence for a doubly magic character of nuclei with Z=20, N=32 and N=34 [3,4]. The experimental measurements performed at ISOLDE led to substantial theoretical efforts to understand the origins of this effect and reproduce it numerically. In this context, several developments were made within different theoretical approaches. In density-functional theory, the overall increase could be reproduced by a modified Fayans functional, albeit with overestimated odd-even staggering [5]. From a shell-model perspective, Bonnard and coworkers found that the rms charge radii beyond N=28, along with mirror energy differences, could be explained if one introduces the concept of "Halo orbits." Here, it was concluded that the extended rms charge radius was due to neutrons filling "the *huge* p3/2 orbit" [6]. Alternatively, it has been concluded from RMF(BCS) studies [7] that deformation plays an important role in describing these charge radii increases.

While measurements of nuclear rms charge radii have helped to map out the striking effects at N=28, the underling microscopic mechanism for these phenomena remains disputed and unclear. Indeed, the very nature of isotopic changes in mean-square charge radii as a collective observable linked to the proton distribution leaves open many possible interpretations for its neutron-number sensitivity.

In comparison, the Bohr Weiskopf effect, ϵ reflects the sensitivity of an atomic system to the spatial distribution of nuclear *magnetization*. This observable possesses some interesting properties when considering the origins of the N=28 charge radii increase. Firstly, only unpaired nucleons contribute to nuclear magnetization and ϵ, thus in a single particle limit it reflects not the distribution of the collective nucleus, but that of the orbital of the last unpaired nucleon. Secondly, in contrast to the coulombic interactions responsible for the atomic observation of rms charge radii, both unpaired protons and neutrons contribute to it on an equal footing. Although sporadic measurements of this effect have been recorded since the 1950's, most [8] are limited to the valley of stability, where magnetic moments and hyperfine structure (HFS) can be recorded with sufficient resolution. Typically, atomic structure calculations are not sufficiently precise to allow the direct extraction of ϵ, however the differential hyperfine anomaly between two isotopes ${}^{A}\Delta^{B} = \frac{1+\epsilon_A}{1+\epsilon_B} - 1 = \frac{g_B\, A_A}{g_A\, A_B} - 1$ can always be determined experimentally based on the measured nuclear g-factors (or magnetic moments) and HFS constants A, and it provides valuable constraints on any given model of the nuclear magnetization distribution.

In recent work we have demonstrated that by performing β-NMR with ^{47}K in a liquid host, the magnetic moment could be determined with sufficient resolution to obtain a well-defined differential hyperfine anomaly, ${}^{39K}\Delta^{47K}$ from which strong constraints could be placed on the composition of the two magnetic moments [9,10]. In the present work we propose to extend these β-NMR measurements to ^{48,49}K, as well as subsequently provide improved hyperfine A factors for ^{47,48,49}K using the laser-rf double resonance technique. With the combination of these measurements, we aim to provide strong constraints on the radial extent of the neutron $p_{3/2}$ orbit. Additionally, we will measure the spectroscopic quadrupole moment of ^{48}K using β-NQR. This will provide an additional independent constraint on the configuration of this nucleus and a view of any possible deformation.

Measurements

Within our team, we have led the developments that allow us to now reach the needed precision. We have already shown that the use of liquid-state β-NMR in combination with conventional NMR and combined quantum-chemistry calculations gives ppm accuracy in the measured magnetic moments and *g*-factors [11]. Recently, this approach was used to determine the *g*-factor of ^{47}K with high precision. We combined this result with the *A*-factor from laser spectroscopy at ISOLDE and *g* and *A* for stable ^{39}K [12]. We have then determined the relatively large hyperfine anomaly of $^{39K}\Delta^{47K}$ and have also obtained its theoretical prediction based on state-of-the-art atomic and nuclear structure theory [9, 10]. Simultaneous comparison of the experimental and theoretical values of the magnetic moments together with the newly established hyperfine anomaly has allowed us to put constraints on the spin and orbital angular momentum contributions to the magnetic moment operator. Furthermore, we have also investigated the importance of 2-body currents in reaching better agreement between measurements and calculations [10].

To determine the hyperfine anomaly between ^{48}K and ^{47,49}K, expected to be several times smaller than $^{39K}\Delta^{47K}$, will require measurements with improved precision for the *g*-factors of ^{48,49}K and *A*-factors of the three above isotopes (see Table 1).

Table 1. Measured magnetic moments and HFS constants of $^{47\text{-}49}$K, together with theoretical predictions of absolute and differential hyperfine anomaly [12]. Our already improved $\mu(^{47}\text{K}) = 1.936\ 182(19)\ \mu_N$ [9, 10].

	I^π	μ (μ_N)	A (MHz)	ε_{theo} (%)	$^{48}\Delta^{x}_{theo}$ (%)
^{47}K	½$^+$	+1.9292 (2) [58]	+3413.2 (3)	-0.126	0.085
^{48}K	1$^-$	-0.8997 (3) [45]	-795.9 (3)	-0.211	-
^{49}K	½$^+$	+1.3386 (8) [40]	+2368.2 (14)	-0.121	0.090

Magnetic-moment and quadrupole-moment measurements:

To measure precisely the ratio of magnetic moments (and g-factors) of ^{47,48,49}K, we will use liquid-state beta-NMR, in the same configuration as we have already done for ^{47}K [9, 10]. To be specific, we will use 50 keV beams of ^{48,49}K (and ^{47}K as the magnetic moment reference) from ISOLDE and neutralize them in our charge-exchange cell. The neutral atoms will be spin-polarised in the 2 m long optical-pumping section in the $s_{1/2}$->$p_{3/2}$ transition (D2 line) at 766.7 nm provided by the newly commissioned VITO laser lab in bldg. 508. Next, the polarised beam will be implanted into a host kept in the middle of our 4.7 T superconducting magnet. Finally, rf excitations will be used for β-NMR studies. When the frequency corresponds to the Larmor frequency of the specific nucleus, a decrease in the beta decay asymmetry will be observed by two beta detectors, one placed at 0° and the other at 180° to the magnetic field direction.

$^{47\text{-}49}$K atoms will be first implanted into a KCl crystal, in which it is easier to determine the approximate Larmor frequency (wide resonance and long relaxation time, e.g. T_1>20 s for spin ½ ^{47}K). Once the Larmor frequency range has been identified, we will change the sample to the ionic liquid EMIM-DCA which we have already employed in the study of ^{47}K (T_1 around 0.5 s) [9]. At VITO, we have already polarised both ^{47}K [9,10] and ^{49}K [13] and we can expect to reach a similar level of polarisation for ^{48}K.

To determine the quadrupole moment Q of ^{48}K, we will use a solid host in the form of a potassium di-hydrogen phosphate (KH_2PO_4) or KDP single crystal with the known electric field gradient, as previously employed in the quadrupole moment measurement of ^{35}K [14]. Quasi-simultaneus exitation of the NQR resonance frequencies will be employed using switched resonant ciruits in order to enhance the β-NQR signal strength.

Hyperfine structure measurements:

The HFS constant A will be determined with laser-rf double resonance spectroscopy which has been already employed on fast beams of stable nuclei [15,16]. Within the ERC Consolidator Grant PresOBEN, we are adjusting the technique to be used with unstable nuclei at the VITO beamline. This technique allows to reach 1-2 orders of magnitude higher precision in measuring HFS because it relies on direct rf excitations within HFS multiplets. In contrast, the precision of laser spectroscopy is limited by the short lifetime of the excited atomic state (10s-100s of ns).

The principle of the technique is shown in Figure 1 and summarised in Table 2. The modified VITO end-station is shown in Figure 2. Here, the neutralised atomic potassium beam from ISOLDE flies through three regions in which sequentially: the atomic state is prepared using laser light, the beam interacts a travelling rf wave to probe the HFS splitting, the laser light is used to probe (read-out) whether the state of the ion/atom has changed under rf excitation.

The potassium isotopes will be used at 20 keV beam energy to maximise the interaction time with the rf (as the resonance width is driven by the transient time of the beam in the rf line), neutralised in the VITO charge exchange cell, and then optically pumped and probed in the atomic D1 line, $s_{1/2}$->$p_{1/2}$ at 770.1 nm also provided by the VITO lasers.

Table 2. Three regions transversed by the ion/neutralised atom beam in the rf-laser double resonance spectroscopy end station at the VITO beamline.

Step	**Where**	**What**	**Aim**
State preparation	Optical pumping (2 m)	Laser tuned to transition from 1st ground-state HFS level to excited state.	Optical pumping: Transfer electron population from that ground-state HFS level to the other. Maximise population of the 2nd HFS level.
Interaction	Rf line (2 m)	Laser off. Travelling rf wave with frequency corresponding to energy between the two ground-state HFS levels. For every new ion/atom bunch rf is changed to go across resonance frequency.	Transfer electrons from the maximally populated HFS level to the pumped-out level. Determine the resonance frequency and from that HFS constant A.
State probing	Optical detection (5 cm)	Laser again on with the same frequency. Excitation of electrons from the 1st HFS level. Detection of resulting fluorescence in optical photomultipliers.	Observe intensity of fluorescence vs rf frequency applied to each bunch. Obtain resonance curve for HFS and from that get A factor.

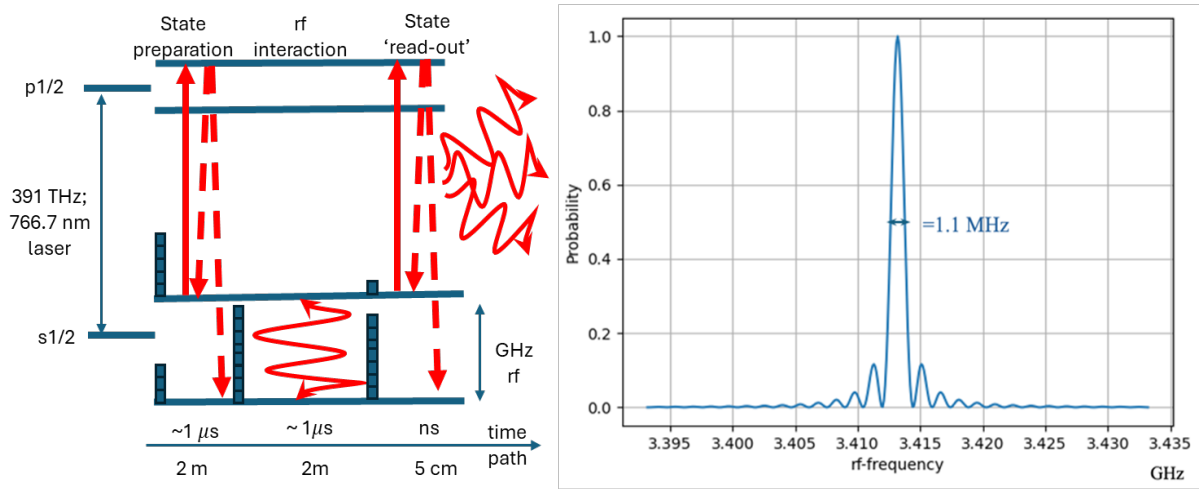

Fig 1. Left: Optical pumping and rf excitation scheme for K atoms in D1 transition. Right: simulated rf resonance shape for ^{47}K, with fit uncertainty expected to be about 10 times smaller than resonance width.

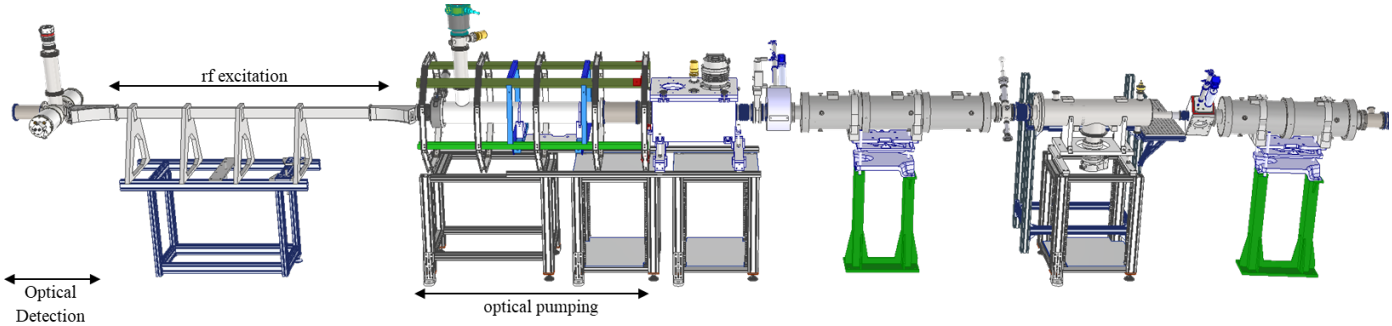

Fig.2. VITO beamline with rf-laser double resonance end station. The ion and laser beam enter from the right. Rf transmission line is to the left, before optical detection region.

The laser-rf spectroscopy endstation will be first commissioned with a beam of stable ^{39}K from ISOLDE with the aim to optimize the transport efficiency, minimize the scattered laser light, determine the approximate rf power needed to transfer all population from one HFS level to another, and finally to determine and optimize the experimental width of resonances, which is governed by the spread in ion beam energy and the homogeneity of rf amplitude across the beam profile. Our rf-beam interaction simulations (Fig. 1 right) show that for the rf coupling as in simulations [15,17], we will require in the range of 1-10 W power at 3-6 GHz. The final measurements will be performed on beams of ^{47,48,49}K.

Beam time estimate and request

We request UC target with surface ionisation, HRS separator, and beam bunching in ISCOOL. The expected yields are:

^{47}K $>10^6$ μC^{-1} ^{48}K 1.3×10^6 μC^{-1} ^{49}K 2.7×10^5 μC^{-1}

As the end station of VITO must be changed between measurements using β-NMR and laser-rf double resonance, the β -NMR and β -NQR measurements should be performed in a separate run to those using laser-rf double resonance. In total, considering the requirement to measure first in solid state samples before moving to EMIM-DCA we request a total of 8 online shifts for the β-NMR measurements of ^{48,49}K. The NQR of ^{48}K will require a further sample change

and reduced signal strength must be anticipated (due to the quadrupole splitting of the resonance into several peaks whose distance is proportional to the quadrupole moment). Therefore, we request a further 4 shifts to determine the quadrupole moment of ^{48}K.

Although laser-rf double resonance has previously been employed in collinear laser spectroscopy, a new setup has been developed for these measurements and we will require around 9 shifts of stable beam to fully characterise and optimize systematics associated with laser power and pulse timing.

Following from the successful commissioning we request a further 9 shifts for the high-resolution measurement of the hyperfine A factors of $^{47-49}$K.

Table 3. Beamtime estimate, based on previous b -NMR studies of ^{47}K at VITO, spin polarisation of ^{49}K at VITO, and laser spectroscopy studies at COLLAPS.

	^{39}K	^{47}K	^{48}K	^{49}K
Beta-NMR: 12 RIB shifts				
Optimise spin-polarisation (laser beam overlap, laser power change) +HFS scan	-	0.5	0.5	0.5
Determine Larmor frequency in KCl crystal	-	0.5	0.5	0.5
Measure precise Larmor frequency in EMIM-DCA ionic liquid	-	1	2	2
Measure quadrupole splitting in non-cubic crystal			4	
Rf-laser spectroscopy: 9 stable + 9 RIB shifts				
Optimisation of: transmission, rf-beam overlap, rf power, experimental steps	9	1	-	-
optimise optical pumping and minimise photon background		1	-	-
Rf scans around HFS resonance		2	2	3

Total: **21** Online shifts split over two beamtimes + **9** shifts offline

References

[1] Garcia Ruiz *et al.* Unexpectedly large charge radii of neutron-rich calcium isotopes. *Nature Phys* **12**, 594–598 (2016)

[2] Koszorús, Á., Yang, X.F., Jiang, W.G. *et al.,* Charge radii of exotic potassium isotopes challenge nuclear theory and the magic character of $N = 32$. *Nature Phys* **17**, 439–443 (2021)

[3] Wienholtz, F., *et al.* Masses of exotic calcium isotopes pin down nuclear forces. *Nature* **498**, 346–349 (2013)

[4] Steppenbeck, D. *et al.* Evidence for a new nuclear 'magic number' from the level structure of ^{54}Ca. *Nature* **502**, 207–210 (2013)

[5] P.-G. Reinhard and W. Nazarewicz, Phys. Rev. C **95**, 064328 (2017)

[6] J. Bonnard, S. M. Lenzi, and A. P. Zuker, Phys. Rev. Lett. **116**, 212501 (2016)

[7] R. An *et al., Chinese Phys. C* **46,** 054101 (2022)

[8] J. Persson, Table of hyperfine anomaly in atomic systems. At. Data Nucl. Data Tables, **101589**, (2023)

[9] M. Jankowski, Development of the β-NMR technique towards the study of hyperfine anomalies in short-lived nuclei, PhD Thesis, TU Darmstadt and CERN (2024); DOI: 10.26083/tuprints-00028014

[10] M. Bissell *et al*, Hyperfine anomaly in short-lived nuclei, to be submitted to Phys. Rev. Lett (2024)

[11] R. Harding *et al.,* Magnetic Moments of Short-Lived Nuclei with Part-per-Million Accuracy: Toward Novel Applications of β-Detected NMR in Physics, Chemistry, and Biology, Phys. Rev. X **10**, 041061 (2021)

[12] J. Papuga *et al*., Shell structure of potassium isotopes deduced from their magnetic moments, Phys. Rev. C **90**(3), 1 (2014)

[13] M. Piersa-Silkowska, ISOLDE workshop and users meeting 2023, https://indico.cern.ch/event/1316940/contributions/5639448/

[14] K. Minamisono *et al.*, Physics Letters B **662**, 389–395 (2008)

[15] M. Van Hove, R. Silverans, Fast beam collinear laser-rf double resonance, Hyperfine Interactions **38**, 773-792 (1987)

[16] W. J. Childs, PHYSICS REPORTS (Review Section of Physics Letters) **211**,113-165 (1992)

[17] D. Havranek, ELECTRONICS FOR SCINTILLATOR DETECTOR READOUT AND COAXIAL RF LINE FOR VITO BEAMLINE AT ISOLDE FACILITY AT CERN, Master thesis, Brno University of Technology (2024), https://dspace.vut.cz/items/71ce4df9-6378-4adf-a388-1d7bcc5ff255

1 Details for the Technical Advisory Committee

3.1 General information

Describe the setup which will be used for the measurement. If necessary, copy the list for each setup used.

☒ Permanent ISOLDE setup: *VITO*

☒ To be used without any modification

☒ To be modified: *Installation of laser-rf double resonance end station*

☐ Travelling setup (*Contact the ISOLDE physics coordinator with details.*)

☐ Existing setup, used previously at ISOLDE: *Specify name and IS-number(s)*

☐ Existing setup, not yet used at ISOLDE: *Short description*

☐ New setup: *Short description*

3.2 Beam production

For any inquiries related to this matter, reach out to the target team and/or RILIS (please do not wait until the last minute!). For Letters of Intent focusing on element (or isotope) specific beam development, this section can be filled in more loosely.

- Requested beams:

Isotope	Production yield in focal point of the separator (/μC)	Minimum required rate at experiment (pps)	$t_{1/2}$
^{47}K	$>10^6$	$>10^6$	17.38 s
^{48}K	1.3×10^6	$>10^6$	6.8 s
^{49}K	2.7×10^5	$>10^5$	1.26 s

- From the ISOLDE yield database
- Target - ion source combination: UCx Surface ionization
- RILIS? No

☐ Special requirements: (*isomer selectivity, LIST, PI-LIST, laser scanning, laser shutter access, etc.*)

- Additional features?

  ☐ Neutron converter: (*for isotopes 1, 2 but not for isotope 3.*)

  ☐ Other: (*quartz transfer line, gas leak for molecular beams, prototype target, etc.*)

- Expected contaminants: *No known problematic contaminants*

- Acceptable level of contaminants: No issues with either β-NMR or optical detection experienced previously.

- Can the experiment accept molecular beams? No

3.4 Shift breakdown

An example can be found below, please adapt to your needs. Copy the table if the beam time request is split over several runs.

Summary of requested shifts:

	^{39}K	^{47}K	^{48}K	^{49}K
Beta-NMR: 12 RIB shifts				
Optimise spin-polarisation (laser beam overlap, laser power change) +HFS scan	-	0.5	0.5	0.5
Determine Larmor frequency in KCl crystal	-	0.5	0.5	0.5
Measure precise Larmor frequency in EMIM-DCA ionic liquid	-	1	2	2
Measure quadrupole splitting in non-cubic crystal			4	
Rf-laser spectroscopy: 9 stable + 9 RIB shifts				
Optimisation of: transmission, rf-beam overlap, rf power, experimental steps	9	1	-	-
optimise optical pumping and minimise photon background		1	-	-
Rf scans around HFS resonance		2	2	3

Total: **21** Online shifts split over two beamtimes + **9** shifts offline

3.5 Health, Safety and Environmental aspects

3.5.1 Radiation Protection

• If radioactive sources are required:

  – Calibration of β detectors